Author Manuscript
Author Manuscript
Author Manuscript
Author Manuscript

HHS Public Access
Author manuscript
Science. Author manuscript; available in PMC 2023 November 23.

Published in final edited form as:
Science. 2023 August 18; 381(6659): 771–778. doi:10.1126/science.adi2436.

Human POT1 protects the telomeric ds-ss DNA junction by capping the 5' end of the chromosome

Valerie M. Tesmer[1], **Kirsten A. Brenner**[1], **Jayakrishnan Nandakumar**[1,*]

[1]Department of Molecular, Cellular and Developmental Biology, University of Michigan; Ann Arbor, 48109, USA

Abstract

POT1 is the 3' single-stranded overhang-binding telomeric protein that prevents an ATR DNA damage response (DDR) at chromosome ends. What precludes the DDR machinery from accessing the telomeric double-stranded-single-stranded junction is unknown. We demonstrate that human POT1 binds this junction by recognizing the phosphorylated 5' end of the chromosome. High-resolution crystallographic structures reveal that the junction is capped by POT1 through a "POT-hole" surface, mutating which compromises junction protection in vitro and telomeric 5'-end definition and DDR suppression in human cells. While both mouse POT1 paralogs bind the single-stranded overhang, POT1a, not POT1b, contains a POT-hole and binds the junction, explaining POT1a's sufficiency for end protection. Our study shifts the paradigm for DDR suppression at telomeres by highlighting the importance of protecting the double-stranded-single-stranded junction.

One-Sentence Summary:

POT1 binds the 5' end of the telomeric ds-ss DNA junction to prevent human chromosome ends from being sensed as DNA damage.

Nucleoprotein complexes called telomeres cap chromosome ends to ensure genome integrity. Human telomeric DNA contains ~10–15 kilobases (kb) of tandem 5'-GGTTAG-3'/3'-CCAATC-5' repeats. Although telomeric DNA is primarily double-stranded (ds), all chromosomes terminate in a 50–500 nucleotide (nt) single-stranded (ss) G-rich telomeric overhang (Fig. 1A, bottom) (1). The six-protein shelterin complex coats telomeric DNA

*Corresponding author. jknanda@umich.edu.
Author contributions:
Conceptualization: VMT, JN
Methodology: VMT, KAB, JN
Investigation: VMT, KAB,
Visualization: VMT, KAB, JN
Funding acquisition: JN
Project administration: VMT, JN
Supervision: VMT, JN
Writing – original draft: VMT, JN
Writing – review & editing: VMT, KAB, JN

Competing interests: The authors do not have any competing interests to declare.

The Supplementary material associated with this paper contain Materials and Methods, Figs. S1 to S13, Tables S1 and S2, and References numbered 44–55).

Author Manuscript Author Manuscript Author Manuscript Author Manuscript

to protect chromosome ends from being recognized as ds DNA breaks by the ataxia telangiectasia and Rad3-related (ATR) kinase- and ataxia-telangiectasia-mutated (ATM) kinase-mediated DNA damage response (DDR) machineries (2, 3). ATR signaling involves multiple protein factors and coordinated recognition of both the ss and the adjacent ds-ss junction of its DNA substrates (4). POT1 (protection of telomeres 1) is a shelterin component that binds the ss G-rich overhang with high affinity and sequence specificity and prevents ATR signaling at telomeres (2, 5, 6). POT1 recognizes ss DNA through its DNA binding domain (DBD) consisting of two oligonucleotide/oligosaccharide-binding (OB) domains (Fig. 1A). Previous studies have reported a decanucleotide within two telomeric ss repeats ^{1}GGTTAG GGTTAG^{12} to be sufficient for high affinity binding to human POT1 (hPOT1) (7). The first OB domain (OB1) of hPOT1 binds ^{3}TTAGGG^{8} (OB1^{DNA}), while its second OB domain (OB2) binds ^{9}TTAG^{12} (OB2^{DNA}) (Fig. 1, A and B) (7). Homologs of POT1 are identifiable across eukaryotes (5, 8–15), and knocking out the POT1 parolog in mice involved in chromosome end protection (POT1a) is embryonic lethal (14, 15).

The current model for ATR suppression at telomeres invokes the prevention of RPA loading to the ss overhang by POT1 via its high affinity for telomeric ss DNA and its tethering to the rest of shelterin at telomeric ds DNA (2, 6, 16). Yet multiple observations suggest additional features of POT1 involved in ATR repression. First, mouse POT1 paralogs POT1a and POT1b display indistinguishable ss DNA-binding activity, but only POT1a is sufficient for chromosome end protection (6, 15, 17) while POT1b regulates chromosome end-processing/replication activities (16, 18–21). Replacing the DBD of POT1b with that of POT1a or hPOT1 enables ATR repression at telomeres (17). Second, replacing the DBD of POT1a with that of ss DNA-binding protein Replication protein A 70 (RPA70) is not sufficient to fully repress ATR signaling at telomeres in mouse cells lacking *POT1a* (16). Finally, POT1's binding to the G-rich ss overhang doesn't explain how it dictates the 5' end of the C-rich strand, which terminates predominantly in ATC-5' in mammals (22, 23) (Fig. 1A, bottom). These observations are consistent with the DBD of hPOT1 and mouse POT1a carrying out an additional function relevant to ATR suppression.

Results

Human POT1 binds a 5'-phosphorylated telomeric ds-ss DNA junction.

We hypothesized that hPOT1 binds to the telomeric ds-ss junction after reanalyzing its published DNA binding site preferences. Two classes of POT1 binding sites emerged from previous SELEX (systematic evolution of ligands by exponential enrichment) analysis, one of which was the expected ^{3}TTAGGGTTAG^{12} (OB1^{DNA}-OB2^{DNA}) site (*Class I*; Fig. 1B) (24). A second class contained OB1^{DNA}, an upstream tri-K (K = T/G), and a seemingly non-telomeric (NT) sequence implicated in binding to OB1 (consensus: CTCCAGCAG*GGG* ^{3}TTAGGG^{8}; *Class II*; Fig. 1B) (24). Junction binding was suspected based on the observation that the tri-K *GGG* motif corresponds to the telomeric repeat sequence upstream of OB1^{DNA}, and NT sequences in the *Class II* hits could fold into a hairpin (hp) containing a two-base-pair (bp) stem $^{-1}$GG^{0}/$^{-6}$CC^{-7} and a variable tetraloop (positions −5 to −2) (Fig. 1B and fig. S1, A and B). In this interpretation, G^{0} and C^{-7} represent the first bp at the ds-ss junction (with C^{-7} corresponding to the 5' end of the

Author Manuscript Author Manuscript Author Manuscript Author Manuscript

mammalian chromosome) and the 3’ overhang initiates in the GGTTAG register (Fig. 1, A and B, and fig. S1, A and B). We conducted a quantitative electrophoretic mobility shift assay (EMSA) with purified hPOT1 DBD (hDBD; fig. S2A) and a 5’ ^{32}P-labeled hp oligonucleotide derived from the *Class II* consensus terminating in a C at the 5’ end and containing a 3’ overhang of sequence $^{\mathbf{1}}$GGTTAGGG$^{\mathbf{8}}$ (hp-ss$^{1-8}$; Fig. 1C). The absence of OB2^{DNA} from the *Class II* consensus attenuates the affinity of hDBD for ss DNA (7), allowing us to assess DNA affinity of POT1 for the ds-ss junction. hDBD bound strongly to hp-ss$^{1-8}$ (K_d = 2.6 ± 0.3 nM) but not to a similar target (no_hp-ss$^{1-8}$) lacking the ability to form a hairpin (Fig. 1, C and D) (7). The natural telomeric ds-ss junction ends in a 5’-phosphate (5’-P), which has been previously exploited to determine the 5’-terminal nt of chromosomes using DNA ligase-mediated methods (25). To test the importance of this phosphate in binding hPOT1, we performed a competition experiment mixing 5’–^{32}P-hp-ss$^{1-8}$ with either non-radiolabeled 5’-phosphorylated hp-ss$^{1-8}$ or 5’-OH-hp-ss$^{1-8}$ before binding to hDBD. The 5’-P was required to effectively outcompete POT1 binding to the radiolabeled DNA (Fig. 1E). The absence of a 5’-P at the DNA junction in past in vitro studies may have prevented the detection of this previously unappreciated POT1 DNA-binding activity (17, 26–29). POT1 bound to a telomeric ds-ss junction in vivo is poised to engage both OB1^{DNA} and OB2^{DNA}. Extension of the overhang of the hp to include OB2^{DNA} (hp-ss$^{1-12}$) resulted in a higher affinity for hDBD (K_d = 70 pM; Fig. 1, C and F) compared with either ss$^{1-12}$ (K_d = 190 pM; Fig. 1C, and fig. S2B) or hp-ss$^{1-8}$ (Fig. 1, C and D). We confirmed that a heterodimer of full-length hPOT1 and shelterin partner TPP1 (using the TPP1N truncation construct), which approximates the context of hPOT1 coating the ss overhang in vivo (30, 31), exhibited robust binding to 5’-P hp-ss$^{1-12}$ (Fig. 1G). DBD bound a two-stranded DNA (duplex reinforced using thirty bp of non-telomeric sequence) terminating in five bp of native ds telomeric junction sequence and an eight nt overhang (long_ds_ss$^{1-8}$) with an affinity that was õne order of magnitude greater than observed with hp-ss$^{1-8}$, likely reflecting the greater stability of the more physiologically representative duplex DNA versus the hp (Fig 1, C and H). Our data demonstrate that the telomeric ds-ss junction is a previously unappreciated high-affinity binding site for hPOT1.

High-resolution structures reveal how human POT1 caps the phosphorylated 5’ end of a telomeric junction.

To determine the structural basis for hPOT1’s telomeric ds-ss junction-binding activity, we formed complexes of hDBD with two substrates that mimic the telomeric ds-ss junction: 5’-P-ds-ss$^{1-12}$ (DNA containing a 5 bp non-telomeric tether upstream of GTTAG/CAATC-5’-P native telomeric ds sequence extending into a twelve nt 3’ overhang; fig. S2, C and D) and 5’-P-hp-ss$^{1-12}$ (Fig. 1C), and solved their structures using X-ray crystallography (Fig. 2, A and B). The hDBD-bound 5’-P-ds-ss$^{1-12}$ and 5’-P-hp-ss$^{1-12}$ structures were solved to 2.60 Å and 2.16 Å resolution, respectively (table S1). Both structures are similar to each other (fig. S3D) and recapitulate the previously reported hDBD-ss DNA-binding interface with minor differences (fig. S3, A–C and E–J) (7). The new structures reveal how hPOT1 binds the phosphorylated 5’-end of the telomeric ds-ss junction (Fig. 2). An electropositive pocket of four amino acids (Y9, R80, H82, and R83) in the hPOT1 OB1 domain that we name the POT-hole caps the 5’-P-cytidine nucleotide using a network of stacking and electrostatic interactions (Fig. 2, D–F, and fig. S4A). R83 acts as the linchpin by forming an

Author Manuscript Author Manuscript Author Manuscript Author Manuscript

ionic interaction with the 5'-P, stacking against the 5'-cytosine base, and forming H-bonds with the ribose ring oxygen of the 5'-cytidine nucleoside (Fig. 2, D and F, and fig. S4A). R83 also forms an H-bond with Y9, which along with H82, interacts with the 5'-P. R80 forms a water-mediated H-bond with the 5'-P. We observe that the POT-hole is not optimally sized to accommodate a bulkier adenine (purine instead of a pyrimidine) or thymine (methyl group on the base) at the 5' end due to steric clashes (fig. S5, A–C). Furthermore, the fixed distance between the POT-hole and the ss DNA-binding region of hPOT1 dictates the preference for the naturally occurring ATC-5' versus alternative 5'-C iterations: ATCC-5' and ATCCC-5' (fig. S5D). In addition to interactions involving the POT-hole, junction recognition is fortified by contacts made by the backbone amides of hPOT1 amino acids (aa) 121–124 with the phosphodiester group penultimate to the 5'-C (Fig. 2F and fig. S4B) as well as S99 with G^2 (fig. S3, K and L). Together, these data provide the structural basis for binding of the telomeric ds-ss junction by hPOT1.

The POT-hole dictates telomeric DNA junction binding and inhibits DDR at telomeres.

We evaluated the importance of the POT-hole in binding the telomeric ds-ss junction in vitro using purified hDBD variants with alanine mutations at Y9, R80, H82, and R83 (fig. S6A). We also engineered an R83E charge reversal mutant to test the importance of the ionic R83–5'-P interaction. Alanine substitution of F62, a residue in hPOT1 OB1 indispensable for binding telomeric ss DNA (32), was included as a control to disrupt binding to both ss DNA and the ds-ss junction. In agreement with the structural data, little to no DNA binding was observed for any POT-hole mutant with the 5'-P-hp-ss^{1-8}, even at concentrations 100-fold higher than the K_d with wild type (WT) hDBD (Fig. 3A, left). In contrast, POT-hole mutants bound 5'-P-ss^{1-12} with an affinity similar to WT (Fig. 3A; fig S6, B and C). F62A failed to bind either oligonucleotide, consistent with binding to $OB1^{DNA}$ being critical for both DNA-binding modes. These data highlight the importance of the POT-hole in 5'-end binding and provide separation of function mutants to test the importance of hPOT1's junction-binding activity in cells (Fig. 3B).

Loss of POT1 binding at the 3' overhang results in telomere-dysfunction-induced foci (TIF), which signify the recognition of telomeres by the DDR machinery (33). To determine the biological importance of the POT-hole binding to the telomeric junction, we used a previously described inducible *POT1* KO cell line (34) and transduced WT and mutant hPOT1 Myc-tagged constructs to test their ability to compensate for the loss of endogenous POT1 (Methods). Transduced cells were treated first with 4-OHT to knockout *POT1* and then either treated with dox to induce exogenous hPOT1 expression ("+dox") or left untreated ("-dox") (Fig. 3C). In the absence of dox, 4-OHT treatment resulted in a robust TIF phenotype, characterized by the co-localization of the DDR factor 53BP1 at telomeres (fig. S6, E and F). hPOT1 WT and "low dox" WT, but not hPOT1 F62A, suppressed TIFs (Fig. 3, D and E). POT-hole mutants Y9A, R83A, and R83E were defective in TIF suppression compared to WT, with R83E being the most deleterious (Fig. 3, D and E). This trend emphasizes the importance of the ionic interaction between R83 and the 5'-P. Clones isolated from 6X-Myc tagged hPOT1 WT, F62A, and R83E cell populations also recapitulated the TIF phenotypes (fig. S7, A–D). Notably, TIFs were smaller (Fig. 3D, Inset) and less frequent (Fig. 3, D and E) in POT-hole mutant cells compared to F62A

Author Manuscript Author Manuscript Author Manuscript Author Manuscript

cells. This suggests that both junction- and ss DNA-binding activities of hPOT1 must be compromised to trigger a full DDR (see Discussion). Our results demonstrate that junction binding, which should involve a single POT1 molecule per chromosome end (Fig. 3B), is critical for chromosome end protection.

The POT-hole differentiates mouse POT1 paralogs and enables POT1a to protect the telomeric junction.

Despite being strictly conserved in other mammalian POT1 homologs, including mouse POT1a, each of the four POT-hole amino acids is replaced with a structurally disparate residue in mouse POT1b (Fig. 4A and fig. S8A). In contrast, the residues involved in ss DNA binding are conserved in all mammalian POT1 homologs, including POT1b (fig. S8A). Aligning Alphafold predictions (35) of POT1a and POT1b DBDs with the junction-bound structure of hDBD illustrates that the shape and the electropositive nature of the POT-hole are predicted to be lost in POT1b (Fig. 4B, and fig. S8, B and C). We hypothesized that POT1a, but not POT1b, protects the 5’ end at the junction. Indeed, POT1a and POT1b DBD proteins bound ss^{1-12}, but only POT1a DBD engaged a telomeric ds-ss junction with high affinity (Fig. 4, C–E, and fig. S8, D and E). POT1a replaced with POT1b residues in the POT-hole (except R80, see fig. S8F for rationale), retained affinity towards ss^{1-12} (Fig. 4C) but failed to bind the junction (Fig. 4, D, right, and E, and fig. S8D).

To measure junction-binding in the presence of multiple ss DNA binding sites, we developed an EMSA-based “POT1 packing” assay with two DNA targets, each containing four telomeric ss repeats (24 nt) spanning three possible POT1-binding registers. The 5’ and 3’ registers are compatible with the packing of two POT1 molecules, whereas binding to a central register precludes the loading of a second POT1 (Fig. 4F, left). hp-ss^{1-24} includes a ds-ss junction upstream of this ss region, while ss^{1-24} does not. A fully packed 2:1 DBD-DNA complex would produce a sharp, slow-migrating band at higher DBD concentrations, while a mix of 2:1 and 1:1 complexes (of various binding registers) would generate a smear. POT1a DBD binding resulted in a sharp band for hp-ss^{1-24} but not ss^{1-24}, suggesting that the protein packs preferentially against a ds-ss junction, but that there is no end-binding bias to dissuade it from binding to the central site of ss^{1-24} (Fig. 4F, right). POT1a POT-hole mutants R83G and triple mutant YHR lost the ability to pack at the junction (Fig. 4G), consistent with R83 capping the 5’ terminus (Fig. 2, D and F) and repressing TIFs (Fig. 3, D and E). hDBD and mouse POT1b DBD formed a discrete complex with not only hp-ss^{1-24} but also ss^{1-24}, consistent with a 3’-end-binding preference (fig. S9, A and B) (7). Our results demonstrate that the POT-hole allows POT1a to preferentially bind the telomeric junction.

The POT-hole helps maintain the 5’-end identity of human chromosomes.

Consistent with the new structures, the POT-hole of hDBD and mouse POT1a DBD protect the 5’-P end from 5’ exonucleolytic action in vitro (fig. S10, A–F). We next asked if the POT-hole helps maintain the 5’-terminal sequence of the chromosomes in cells. We used a modified Single Telomere Length Analysis (STELA) approach that employs ligation-mediated PCR amplification to determine the abundance of each of the six possible chromosomal 5’-end permutations (23) (Fig. 5A). Genomic DNA extracted

Author Manuscript Author Manuscript Author Manuscript Author Manuscript

from the parental HEK 293E cell line displayed the expected ATC-5’ preference that is lost following *POT1* KO (Fig. 5, B and C). WT hPOT1, but not R83E hPOT1, was able to restore the ATC-5’ bias to untreated (parental −4-OHT) levels, demonstrating that the POT-hole helps maintain the 5’ end of the human chromosome (Fig. 5, B and C, and fig. S10G). The 5’ end-scrambling of hPOT1 R83E was less severe than that of the knockout. This difference may be explained by the ATR signaling-mediated unleashing of 5’ exonuclease activity at telomeres completely devoid of POT1 (36). Telomere restriction fragment (TRF) analysis reproduced previously characterized phenotypes (15, 34, 37), including the accumulation of slow-migrating species (denatured and native blots) and an increase in G-rich ss signal (native blot) upon *POT1* KO, which were suppressed by expression of hPOT1 WT but not F62A (Fig. 5D and fig. S10H). R83E recapitulated the WT phenotypes, suggesting that the end protection function of the POT-hole is separable from hPOT1’s role in bulk telomere or overhang length maintenance. Thus, the POT-hole helps maintain ATC-5’ ends without significantly influencing telomere length.

Discussion

The major pathway of ATR activation requires RPA binding to exposed ss DNA and recognition of the ds-ss junction by the 9–1-1/Rad17-RFC (RAD9–RAD1–HUS1/Rad17-RFC2–RFC3–RFC4–RFC5) clamp/clamp loader, which with the MRN (MRE11-RAD50-NBS1) complex recruits TOPBP1 to activate ATR (4, 38) (Fig. 5E). The structure of human 9–1-1/Rad17-RFC bound to a ds-ss junction revealed a basic pocket in Rad17 that is poised to bind the 5’-phosphorylated end of a junction using a mechanism similar to that of POT1 (fig. S11, A and B) (39). Consistent with a competition between POT1 and 9–1-1/Rad17-RFC in binding the ds-ss junction, subunits of the 9–1-1 and MRN complexes as well as TOPBP1 are enriched at telomeres in the absence of hPOT1 (34). We, therefore, propose that POT1 not only out-competes RPA at the telomeric ss overhang but also prevents ATR activation by denying 9–1-1/Rad17-RFC access to the telomeric ds-ss junction (Fig. 5E).

The duplication of POT1 (40), the conservation of the POT-hole in POT1a (fig. S12A), the disruption of the POT1-hole in POT1b (fig. S12B), and the retention of CST-binding motifs in POT1b (40) within the Muridae and Cricetidae families of the Rodentia order provide support to the hypothesis that POT1b relinquished junction binding to facilitate processes at the 3’ end. We propose that POT1a wards off 9–1-1/Rad17-RFC at the junction although both POT1a and POT1b paralogs could counter RPA at the overhang in mouse cells (Fig. 5E).

The POT-hole is conserved in species distant to mammals, such as *S. nova* and *C. elegans* (fig. S13A). The precisely defined *S. nova* macronuclear telomere contains a 5’-C at the ds-ss junction and a 16 nt overhang that binds one TEBPα/β complex (homologous to the POT1-TPP1 complex) (41). TEBPα has been crystallized with a sulfate ion bound in a manner indistinguishable from how the 5’-P binds hDBD in our junction-bound structures (fig. S13B) (42). Indeed, like hPOT1, TEBPα was shown to bind the telomeric ds-ss junction more strongly than telomeric ss DNA (8). Taken together, these observations point to a single TEBPα/β complex simultaneously protecting the 5’ and 3’ ends of the chromosome (8, 41, 42). *S. pombe*, in which a POT-hole is not obvious (fig. S13, A and

Author Manuscript Author Manuscript Author Manuscript Author Manuscript

C) (5, 43), and eukaryotes whose chromosomes don't end in a 5'-C, must have evolved alternative approaches for junction protection.

We update the model for how telomeres avert detection by the DDR machinery to include a critical role of POT1 in binding the telomeric ds-ss junction. Thus, POT1 protects both DNA strands at human chromosome ends by coating the G-rich ss overhang and recognizing the phosphorylated 5' end of the C-rich strand.

Supplementary Material

Refer to Web version on PubMed Central for supplementary material.

Acknowledgments:

We thank Shilpa Padmanaban (Nandakumar laboratory) for input on the design of the cell-based experiments; Dr. Galina Glousker and Dr. Joachim Lingner (Ecole Polytechnique Fédérale de Lausanne (EPFL), Switzerland) for graciously gifting the *POT1* inducible KO HEK 293E cell line and the pCW22_TREtight_MCS_UBC_rtTA_IRES_Blast lentiviral vector for dox-inducible expression, and for sharing detailed protocols and troubleshooting tips for these resources; Dr. Jens Schmidt (Michigan State University, USA) for the 53BP1 antibody; the beamline staff at the Life Sciences Collaborative Access Team (LS-CAT) beamline of the Argonne National Laboratory for help with X-ray diffraction data collection (use of the Advanced Photon Source, an Office of Science User Facility operated for the U.S. Department of Energy (DOE) Office of Science by Argonne National Laboratory, was supported by the U.S. DOE under Contract No. DE-AC02-06CH11357); Frances Caroline Lowder and Dr. Lyle Simmons (University of Michigan at Ann Arbor, USA) for helpful suggestions regarding the exonuclease protection experiment using fluorophore-labeled DNA and preparation of an RNA ladder; Dr. Titia de Lange and Sarah Cai (Rockefeller University, USA), Dr. Jens Schmidt (Michigan State University, USA), Dr. Hiroki Shibuya (University of Gothenburg, Sweden), and Jonathan Williams (Nandakumar laboratory) for helpful comments on the manuscript; and Gregg Sobocinski for help with microscopy.

Funding:

National Institutes of Health grant R01GM120094 (J.N.)

National Institutes of Health grant R01HD108809 (J.N.)

National Institutes of Health grant R35GM148276 (J.N.)

American Cancer Society Research Scholar grant RSG-17-037-01-DMC (J.N.)

Data and materials availability:

All data are available in the main and supplementary figures. All new material generated in this study such as plasmids for protein expression and cell lines are available upon request. Coordinates and structure factors of the crystal structures of hDBD with 5'-P-hp-ss$^{1-12}$ and 5'-P-ds-ss$^{1-12}$ are deposited in the protein data bank (PDB) under the accession codes 8SH0 and 8SH1, respectively.

References and Notes

1. Palm W, de Lange T, How shelterin protects mammalian telomeres. Annu Rev Genet 42, 301–334 (2008). [PubMed: 18680434]
2. Denchi EL, de Lange T, Protection of telomeres through independent control of ATM and ATR by TRF2 and POT1. Nature 448, 1068–1071 (2007). [PubMed: 17687332]
3. de Lange T, Shelterin-Mediated Telomere Protection. Annu Rev Genet 52, 223–247 (2018). [PubMed: 30208292]

Author Manuscript Author Manuscript Author Manuscript Author Manuscript

4. Saldivar JC, Cortez D, Cimprich KA, The essential kinase ATR: ensuring faithful duplication of a challenging genome. Nat Rev Mol Cell Biol 18, 622–636 (2017). [PubMed: 28811666]
5. Baumann P, Cech TR, Pot1, the putative telomere end-binding protein in fission yeast and humans. Science 292, 1171–1175 (2001). [PubMed: 11349150]
6. Gong Y, de Lange T, A Shld1-controlled POT1a provides support for repression of ATR signaling at telomeres through RPA exclusion. Mol Cell 40, 377–387 (2010). [PubMed: 21070964]
7. Lei M, Podell ER, Cech TR, Structure of human POT1 bound to telomeric single-stranded DNA provides a model for chromosome end-protection. Nat Struct Mol Biol 11, 1223–1229 (2004). [PubMed: 15558049]
8. Gottschling DE, Zakian VA, Telomere proteins: specific recognition and protection of the natural termini of Oxytricha macronuclear DNA. Cell 47, 195–205 (1986). [PubMed: 3094961]
9. Price CM, Cech TR, Telomeric DNA-protein interactions of Oxytricha macronuclear DNA. Genes Dev 1, 783–793 (1987). [PubMed: 3123321]
10. Horvath MP, Schweiker VL, Bevilacqua JM, Ruggles JA, Schultz SC, Crystal structure of the Oxytricha nova telomere end binding protein complexed with single strand DNA. Cell 95, 963–974 (1998). [PubMed: 9875850]
11. Nugent CI, Hughes TR, Lue NF, Lundblad V, Cdc13p: a single-strand telomeric DNA-binding protein with a dual role in yeast telomere maintenance. Science 274, 249–252 (1996). [PubMed: 8824190]
12. Lin JJ, Zakian VA, The Saccharomyces CDC13 protein is a single-strand TG1–3 telomeric DNA-binding protein in vitro that affects telomere behavior in vivo. Proc Natl Acad Sci U S A 93, 13760–13765 (1996). [PubMed: 8943008]
13. Raices M et al. , C. elegans telomeres contain G-strand and C-strand overhangs that are bound by distinct proteins. Cell 132, 745–757 (2008). [PubMed: 18329362]
14. Wu L et al. , Pot1 deficiency initiates DNA damage checkpoint activation and aberrant homologous recombination at telomeres. Cell 126, 49–62 (2006). [PubMed: 16839876]
15. Hockemeyer D, Daniels JP, Takai H, de Lange T, Recent expansion of the telomeric complex in rodents: Two distinct POT1 proteins protect mouse telomeres. Cell 126, 63–77 (2006). [PubMed: 16839877]
16. Kratz K, de Lange T, Protection of telomeres 1 proteins POT1a and POT1b can repress ATR signaling by RPA exclusion, but binding to CST limits ATR repression by POT1b. J Biol Chem 293, 14384–14392 (2018). [PubMed: 30082315]
17. Palm W, Hockemeyer D, Kibe T, de Lange T, Functional dissection of human and mouse POT1 proteins. Mol Cell Biol 29, 471–482 (2009). [PubMed: 18955498]
18. Gu P et al. , Distinct functions of POT1 proteins contribute to the regulation of telomerase recruitment to telomeres. Nature communications 12, 5514 (2021).
19. Chen LY, Redon S, Lingner J, The human CST complex is a terminator of telomerase activity. Nature 488, 540–544 (2012). [PubMed: 22763445]
20. Wu P, Takai H, de Lange T, Telomeric 3’ Overhangs Derive from Resection by Exo1 and Apollo and Fill-In by POT1b-Associated CST. Cell 150, 39–52 (2012). [PubMed: 22748632]
21. Wan M, Qin J, Songyang Z, Liu D, OB fold-containing protein 1 (OBFC1), a human homolog of yeast Stn1, associates with TPP1 and is implicated in telomere length regulation. J Biol Chem 284, 26725–26731 (2009). [PubMed: 19648609]
22. Hockemeyer D, Sfeir AJ, Shay JW, Wright WE, de Lange T, POT1 protects telomeres from a transient DNA damage response and determines how human chromosomes end. EMBO J 24, 2667–2678 (2005). [PubMed: 15973431]
23. Sfeir AJ, Chai W, Shay JW, Wright WE, Telomere-end processing the terminal nucleotides of human chromosomes. Mol Cell 18, 131–138 (2005). [PubMed: 15808515]
24. Choi KH et al. , The OB-fold domain 1 of human POT1 recognizes both telomeric and non-telomeric DNA motifs. Biochimie 115, 17–27 (2015). [PubMed: 25934589]
25. Baird DM, Rowson J, Wynford-Thomas D, Kipling D, Extensive allelic variation and ultrashort telomeres in senescent human cells. Nat Genet 33, 203–207 (2003). [PubMed: 12539050]

Author Manuscript Author Manuscript Author Manuscript Author Manuscript

26. Lim CJ, Zaug AJ, Kim HJ, Cech TR, Reconstitution of human shelterin complexes reveals unexpected stoichiometry and dual pathways to enhance telomerase processivity. Nature communications 8, 1075 (2017).
27. Paul T, Liou W, Cai X, Opresko PL, Myong S, TRF2 promotes dynamic and stepwise looping of POT1 bound telomeric overhang. Nucleic Acids Res 49, 12377–12393 (2021). [PubMed: 34850123]
28. Ray S, Bandaria JN, Qureshi MH, Yildiz A, Balci H, G-quadruplex formation in telomeres enhances POT1/TPP1 protection against RPA binding. Proc Natl Acad Sci U S A 111, 2990–2995 (2014). [PubMed: 24516170]
29. Zinder JC et al. , Shelterin is a dimeric complex with extensive structural heterogeneity. Proc Natl Acad Sci U S A 119, e2201662119 (2022).
30. Wang F et al. , The POT1-TPP1 telomere complex is a telomerase processivity factor. Nature 445, 506–510 (2007). [PubMed: 17237768]
31. Nandakumar J et al. , The TEL patch of telomere protein TPP1 mediates telomerase recruitment and processivity. Nature 492, 285–289 (2012). [PubMed: 23103865]
32. He H et al. , POT1b protects telomeres from end-to-end chromosomal fusions and aberrant homologous recombination. EMBO J 25, 5180–5190 (2006). [PubMed: 17053789]
33. Takai H, Smogorzewska A, de Lange T, DNA damage foci at dysfunctional telomeres. Curr Biol 13, 1549–1556 (2003). [PubMed: 12956959]
34. Glousker G, Briod AS, Quadroni M, Lingner J, Human shelterin protein POT1 prevents severe telomere instability induced by homology-directed DNA repair. EMBO J 39, e104500 (2020). [PubMed: 33073402]
35. Jumper J et al. , Highly accurate protein structure prediction with AlphaFold. Nature 596, 583–589 (2021). [PubMed: 34265844]
36. Kibe T, Zimmermann M, de Lange T, TPP1 Blocks an ATR-Mediated Resection Mechanism at Telomeres. Mol Cell 61, 236–246 (2016). [PubMed: 26778124]
37. Loayza D, De Lange T, POT1 as a terminal transducer of TRF1 telomere length control. Nature 423, 1013–1018 (2003). [PubMed: 12768206]
38. MacDougall CA, Byun TS, Van C, Yee MC, Cimprich KA, The structural determinants of checkpoint activation. Genes Dev 21, 898–903 (2007). [PubMed: 17437996]
39. Day M, Oliver AW, Pearl LH, Structure of the human RAD17-RFC clamp loader and 9–1-1 checkpoint clamp bound to a dsDNA-ssDNA junction. Nucleic Acids Res 50, 8279–8289 (2022). [PubMed: 35819203]
40. Myler LR et al. , The evolution of metazoan shelterin. Genes Dev 35, 1625–1641 (2021). [PubMed: 34764137]
41. Klobutcher LA, Swanton MT, Donini P, Prescott DM, All gene-sized DNA molecules in four species of hypotrichs have the same terminal sequence and an unusual 3’ terminus. Proc Natl Acad Sci U S A 78, 3015–3019 (1981). [PubMed: 6265931]
42. Classen S, Ruggles JA, Schultz SC, Crystal structure of the N-terminal domain of Oxytricha nova telomere end-binding protein alpha subunit both uncomplexed and complexed with telomeric ssDNA. J Mol Biol 314, 1113–1125 (2001). [PubMed: 11743727]
43. Lei M, Podell ER, Baumann P, Cech TR, DNA self-recognition in the structure of Pot1 bound to telomeric single-stranded DNA. Nature 426, 198–203 (2003). [PubMed: 14614509]
44. Grill S, Tesmer VM, Nandakumar J, The N Terminus of the OB Domain of Telomere Protein TPP1 Is Critical for Telomerase Action. Cell reports 22, 1132–1140 (2018). [PubMed: 29386102]
45. Mossessova E, Lima CD, Ulp1-SUMO crystal structure and genetic analysis reveal conserved interactions and a regulatory element essential for cell growth in yeast. Mol Cell 5, 865–876 (2000). [PubMed: 10882122]
46. Grill S et al. , TPP1 mutagenesis screens unravel shelterin interfaces and functions in hematopoiesis. JCI Insight, (2021).
47. Battye TG, Kontogiannis L, Johnson O, Powell HR, Leslie AG, iMOSFLM: a new graphical interface for diffraction-image processing with MOSFLM. Acta Crystallogr D Biol Crystallogr 67, 271–281 (2011). [PubMed: 21460445]

Author Manuscript Author Manuscript Author Manuscript Author Manuscript

48. Winn MD et al. , Overview of the CCP4 suite and current developments. Acta Crystallogr D Biol Crystallogr 67, 235–242 (2011). [PubMed: 21460441]

49. McCoy AJ et al. , Phaser crystallographic software. J Appl Crystallogr 40, 658–674 (2007). [PubMed: 19461840]

50. Liebschner D et al. , Macromolecular structure determination using X-rays, neutrons and electrons: recent developments in Phenix. Acta Crystallogr D Struct Biol 75, 861–877 (2019). [PubMed: 31588918]

51. Emsley P, Cowtan K, Coot: model-building tools for molecular graphics. Acta Crystallogr D Biol Crystallogr 60, 2126–2132 (2004). [PubMed: 15572765]

52. DeLano WL, The PyMOL Molecular Graphics System (DeLano Scientific, Palo Alto, CA). (1998).

53. Grill S et al. , Two Separation-of-Function Isoforms of Human TPP1 Dictate Telomerase Regulation in Somatic and Germ Cells. Cell reports 27, 3511–3521 e3517 (2019). [PubMed: 31216472]

54. Herbert BS, Shay JW, Wright WE, Analysis of telomeres and telomerase. Curr Protoc Cell Biol Chapter 18, Unit 18 16 (2003).

55. Nandakumar J, Podell ER, Cech TR, How telomeric protein POT1 avoids RNA to achieve specificity for single-stranded DNA. Proc Natl Acad Sci U S A 107, 651–656 (2010). [PubMed: 20080730]

Author Manuscript Author Manuscript Author Manuscript Author Manuscript

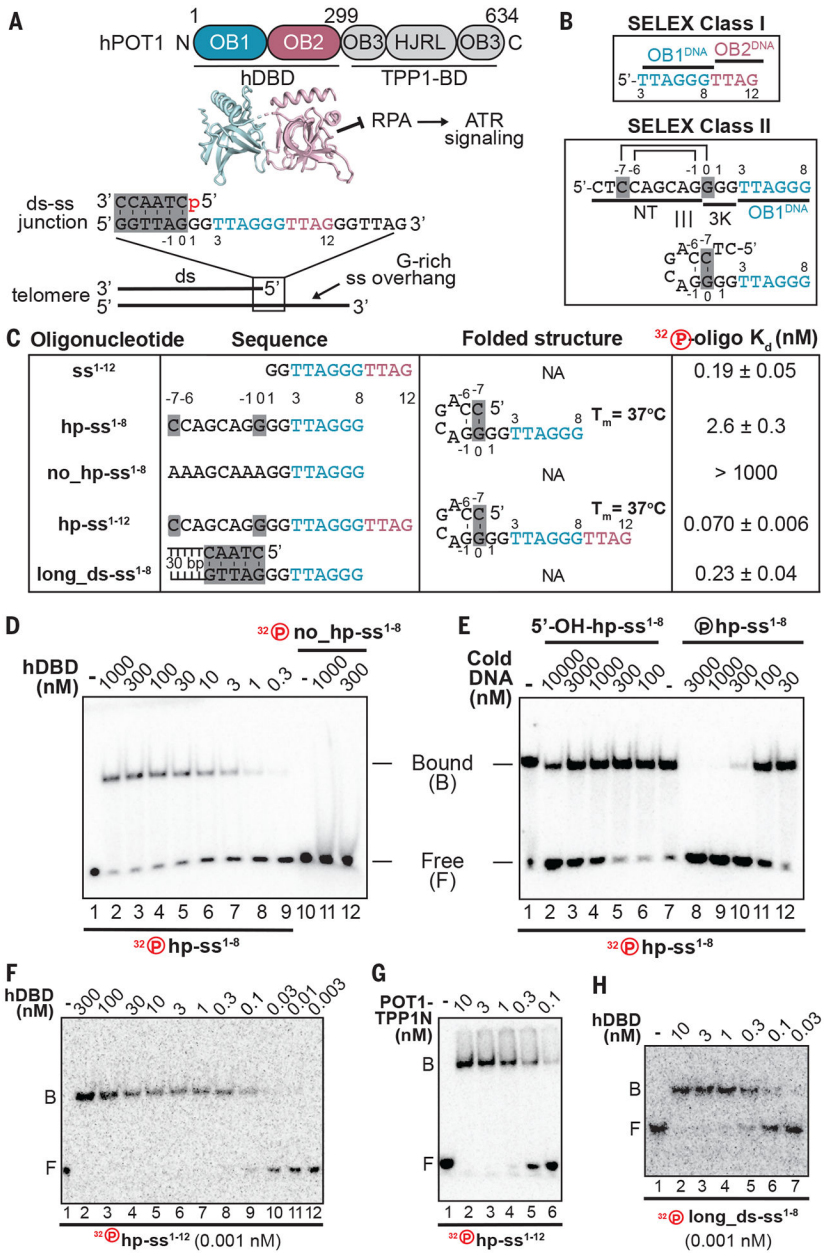

Fig. 1. Human POT1 recognizes the 5'-phosphorylated ds-ss junction of telomeres.

(**A**) *Top:* Schematic of hPOT1 includes binding domains for ss DNA (hDBD) and TPP1 (TPP1-BD). hDBD (PDB: 1XJV) is composed of OB1 and OB2. The current model suggests that POT1 outcompetes the ss DNA-binding RPA complex to prevent ATR signaling at telomeres. *Bottom:* Mammalian chromosomes end in a ds-ss junction containing ATC-5' (predominantly) and a ss G-rich overhang. Numbering starts with the first overhang nucleotide. (**B**) A previous SELEX study revealed two hPOT1-binding DNA classes (24). *Class I* harbors the known sites for OB1 and OB2, denoted as $OB1^{DNA}$ (cyan) and $OB2^{DNA}$ (pink), respectively. *Class II* revealed a novel consensus containing a seemingly non-telomeric (NT) sequence upstream of $OB1^{DNA}$ that can potentially fold into a hp; K indicates G or T nucleotide and the shaded area indicates sequence of the first base

Author Manuscript Author Manuscript Author Manuscript Author Manuscript

pair at the telomeric ds-ss junction. (**C**) Annotated name, sequence, predicted hp structure (with T_m calculated by UNAfold web server), and mean dissociation constant (K_d) and SD (of binding to hDBD) of the oligonucleotides used in EMSA analysis; NA indicates not applicable. (**D**-**H**) EMSA of indicated proteins (hDBD or POT1-TPP1N heterodimer) and 5'–^{32}P-labeled DNA oligonucleotides. D, F, G, and H represent direct binding experiments while E represents a competition experiment. (D) 0.1 nM 5'–^{32}P- hp-ss$^{1-8}$ was used; n=5 for hp-ss$^{1-8}$ (full and partial titrations); and n=3 for no_hp-ss$^{1-8}$. (E) 100 nM hDBD and 0.1 nM 5'–^{32}P-labeled hp-ss$^{1-8}$ were incubated with indicated amounts of unlabeled hp-ss$^{1-8}$ (cold DNA) containing either a 5'-OH or a 5'-P; n=3. (F) 0.001 nM 5'–^{32}P- hp-ss$^{1-12}$ was used; n=3. (G) 0.01 nM 5'–^{32}P- hp-ss$^{1-12}$ was used; n=3. (H) 0.001 nM 5'–^{32}P-long_ds-ss$^{1-8}$ was used; n=3. Circled "P" in red indicates radiolabeled and black indicates non-radiolabeled. Bound or "B" indicates DNA bound to protein and Free or "F" indicates free, unbound DNA.

Author Manuscript Author Manuscript Author Manuscript Author Manuscript

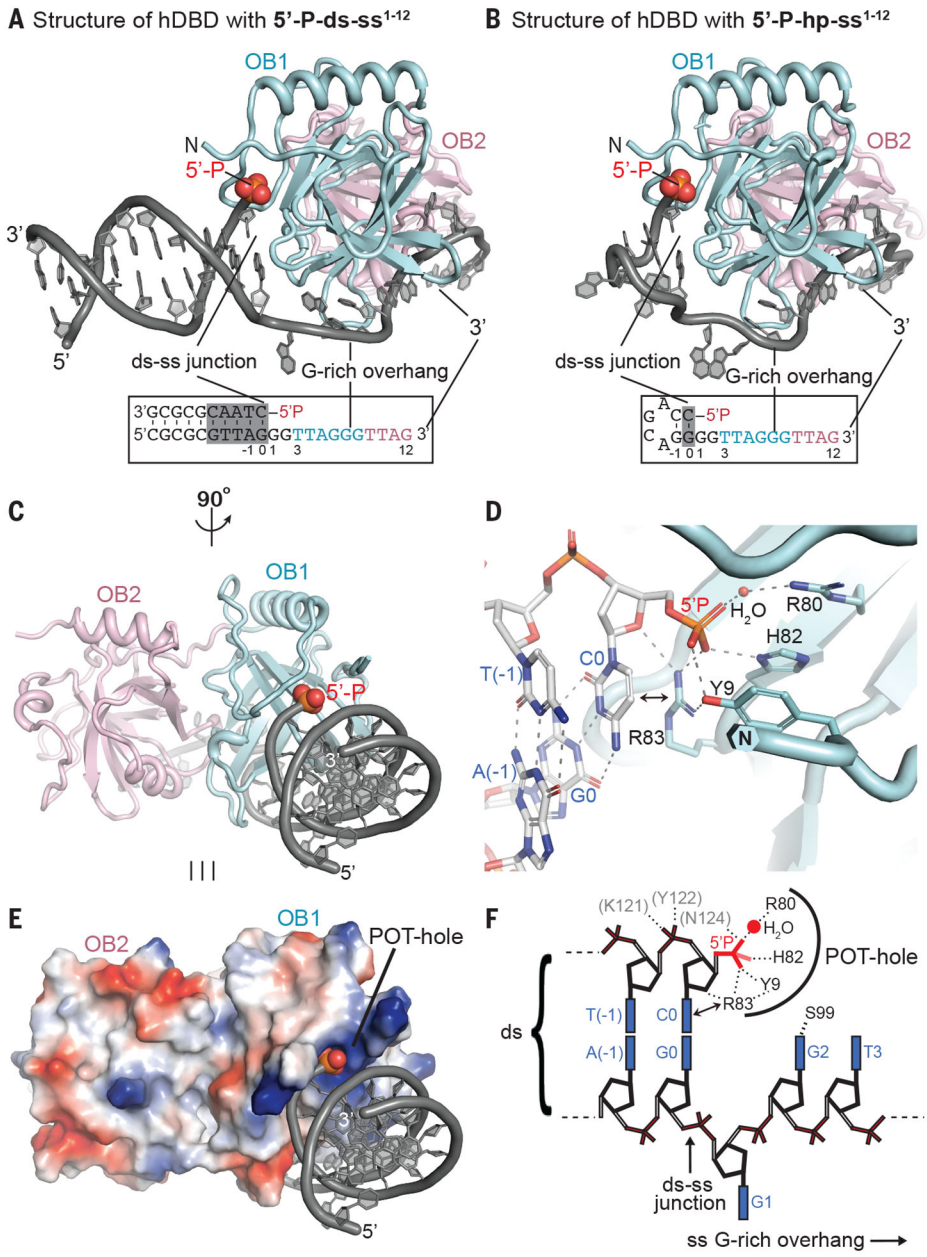

Fig. 2. Structural basis of telomeric junction 5' end protection by human POT1.

(**A** and **B**) Cartoon representation of high-resolution crystal structures of complexes of hDBD with 5'-P-ds-ss$^{1-12}$ (A) and 5'-P-hp-ss$^{1-12}$ (B) showing OB1 (cyan) and OB2 (pink) bound to DNA (grey, with the exception of the 5'-P, whose atoms are shown as spheres and in CPK coloring). A boxed schematic of the DNA is shown below the structure, with the ds sequence found naturally at the telomeric ds-ss junction shaded grey, the 5'-P in red, and residues in the G-rich 3' overhang colored to indicate binding by OB1 and OB2, respectively. (**C** and **E**) Cartoon (C) and electrostatic surface (E; blue is electropositive and red is electronegative) representations of the hDBD-5'-P-ds-ss$^{1-12}$ structure shown in a view orthogonal to that in A. The 5'-P occupies a pocket in POT1 that is complementary in shape and charge. (**D**) The POT-hole-DNA interface within the hDBD-5'-P-hp-ss$^{1-12}$ structure is

Author Manuscript Author Manuscript Author Manuscript Author Manuscript

shown with POT-hole sidechains (carbon in cyan) and the nucleotides (carbon in light grey) near the junction shown as sticks. A water molecule bridging hPOT1 R80 to the 5'-P is shown as a red sphere. Dashed lines: H-bonds and ionic interactions, double-headed arrow: stacking of the hPOT1 R83 sidechain with the 5'-C at the junction (numbered C0), and N indicates the N-terminus of hDBD resolved in the crystal structure. (**F**) Interaction map of hDBD with the ds-ss junction.

Author Manuscript Author Manuscript Author Manuscript Author Manuscript

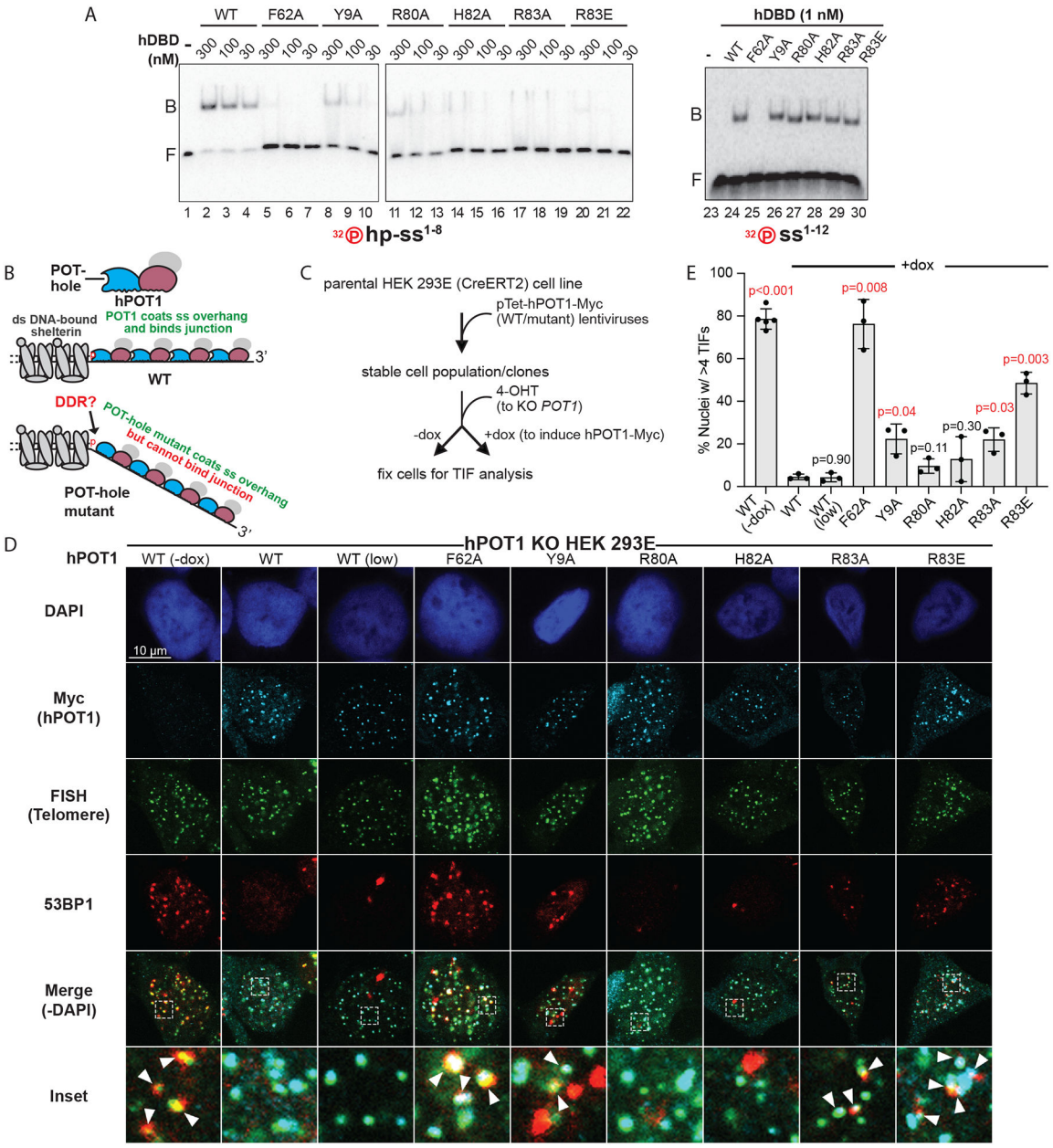

Fig. 3. Separation of function POT-hole mutations abrogate ds-ss DNA junction binding in vitro and result in a DDR at human telomeres.

(A) EMSA to detect direct binding of WT or indicated mutant hDBD constructs with 5'–^{32}P-hp-ss$^{1-8}$ (0.1 nM; lanes 1–22) and 5'–^{32}P-ss$^{1-12}$ (0.1 nM; lanes 23–30); n=3. (**B**) Schematic conveying how POT-hole mutants would disrupt binding to the ds-ss junction but not coating of the ss overhang by POT1. (**C**) Scheme for KO of endogenous *POT1* and complementation with lentivirally transduced hPOT1-Myc to assess the ability of mutants to prevent TIF formation in a HEK 293E-based cell line. (**D**) TIF analysis of cell lines after 4-OHT and dox (1000 ng/ml; 25 ng/ml in 'WT (low)') treatment as described in C using PNA-FISH for telomeres (green) and IF for Myc (hPOT1; cyan) and 53BP1 (red). DAPI was used to stain the nucleus (blue). Overlap of the telomeric and 53BP1 foci in the

Author Manuscript Author Manuscript Author Manuscript Author Manuscript

"Merge" panel (DAPI panel not included) indicates TIFs. Inset shows a magnified view of the boxed area within the image and arrowheads indicate TIFs. (**E**) Quantitation of TIF data of which D is representative. Mean and SD (n=3 for all conditions except WT -dox, for which n=5; each +dox set containing >75 nuclei and -dox set containing >50 nuclei) for TIFs are plotted for the indicated cell lines. P-values calculated using a two-tailed Student's t-test for comparisons against WT +dox data are indicated above the bars.

Author Manuscript Author Manuscript Author Manuscript Author Manuscript

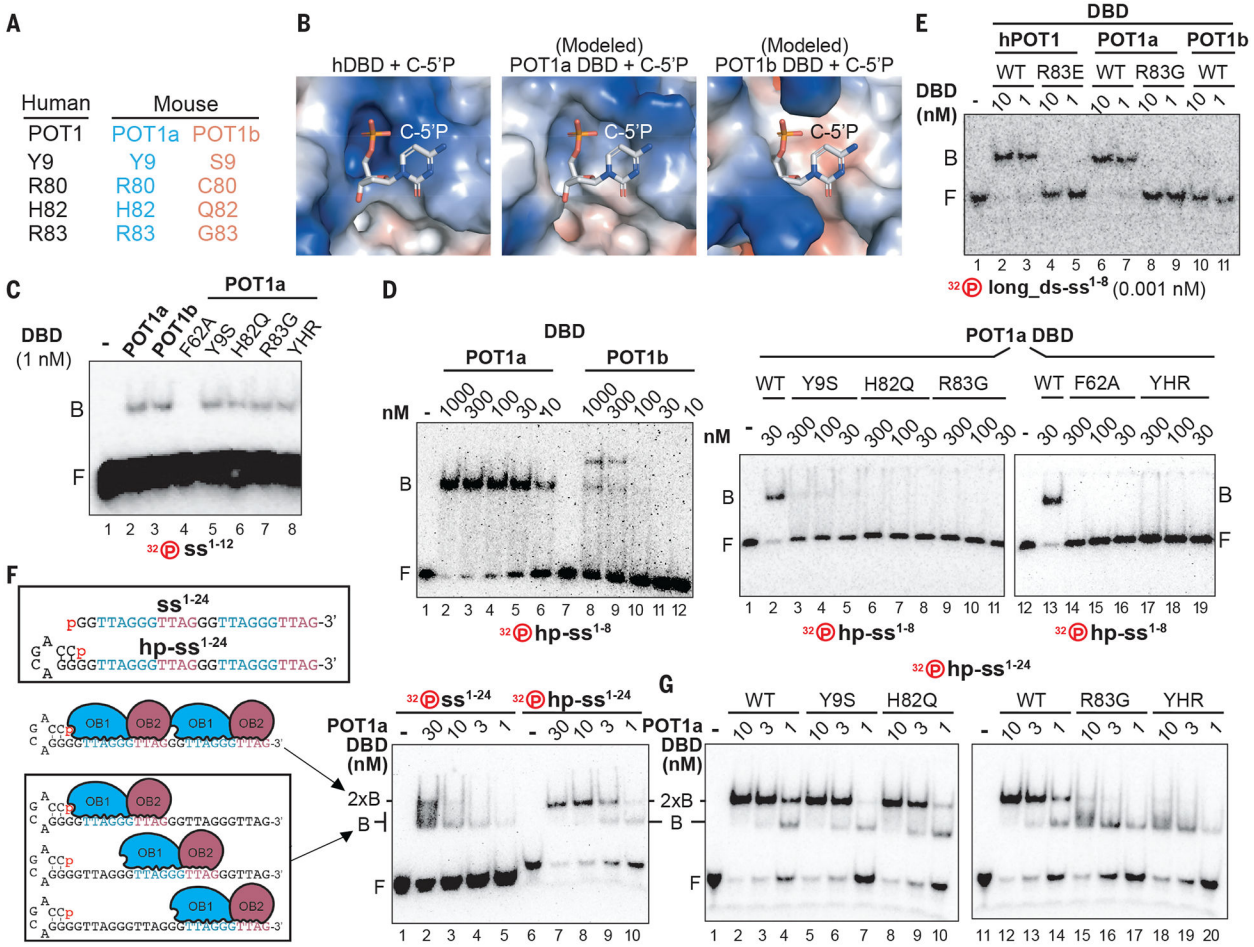

Fig. 4. Presence of the POT-hole dictates POT1 paralog choice for chromosome end protection in mice.

(**A**) Human POT-hole residues are conserved in mouse POT1a but not mouse POT1b. (**B**) Electrostatic surface comparisons of hDBD (from hDBD-5'-P-ds-ss$^{1-12}$ structure) and POT1a and POT1b DBD (Alphafold models) with the phosphorylated 5'-C of the hDBD-bound structure shown in sticks. (**C** and **D**) EMSA analysis of indicated mouse POT1a and POT1b DBD constructs with the indicated 5'–^{32}P-labeled oligonucleotides (0.1 nM for C and D, *right*; 0.01 nM for D, *left*); n=3. (**E**) EMSA analysis of indicated human and mouse POT1 DBD constructs with 0.001 nM 5'–^{32}P- long_ds-ss$^{1-8}$ two-stranded DNA; n=3 (**F**) *Top left:* Names and sequences of the two DNA oligonucleotides, hp-ss$^{1-24}$ and ss$^{1-24}$, used to evaluate 5'-end-binding preference. Both DNAs were labeled at the 5' end with ^{32}P for EMSA analysis. *Bottom left*: Three possible DNA-binding registers for the first DBD molecule are shown with the center-binding register precluding the binding of a second DBD molecule. *Right:* EMSA analysis of POT1a DBD with hp-ss$^{1-24}$ (discrete slow-migrating band with increasing concentrations of protein; 2xB) and ss$^{1-24}$ (smeary band; mixture of B and 2xB), DNA at 0.1 nM; n=3. (**G**) EMSA analysis of indicated POT1a DBD constructs with 0.1 nM hp-ss$^{1-24}$; YHR: triple mutant Y9S-H82Q-R83G; n=3.

Author Manuscript Author Manuscript Author Manuscript Author Manuscript

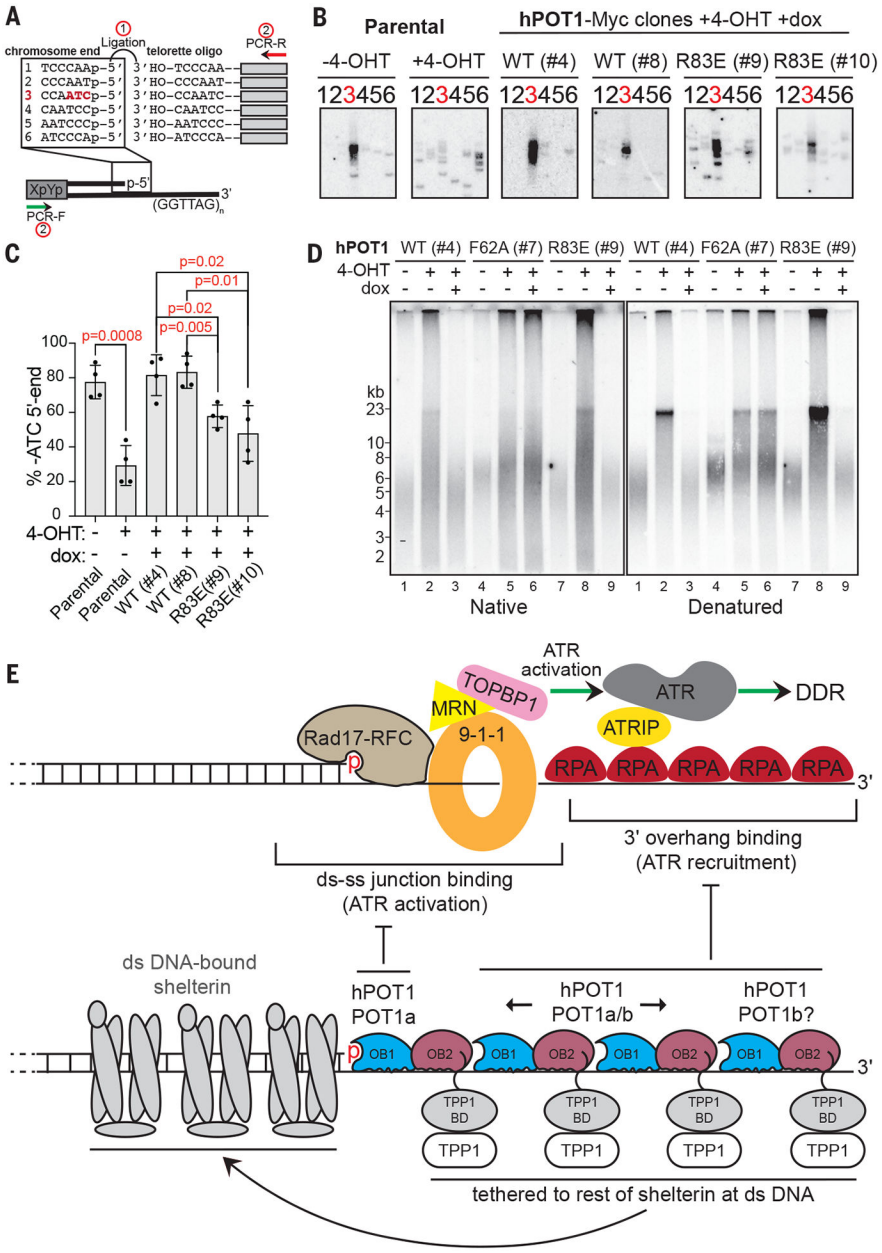

Fig. 5. Maintenance of the ATC-5'end of chromosomes by the POT-hole.

(**A**) Schematic of the modified STELA technique for determining the chromosomal 5'-terminal nucleotide in human cell lines. Step 1 involves DNA ligation of genomic DNA 5'-P ends with telorettes ending in each of the six possible repeat registers at the 3'-OH ends. Step 2 involves PCR amplification of the ligation products using a forward primer targeting the sub-telomere of chromosome XpYp and a reverse primer targeting a sequence shared by all telorettes. The products are visualized using Southern blot analysis using a 5'–^{32}P-labeled XpYpB2 reverse primer. (**B**) STELA-based determination of the chromosomal 5'-terminal nucleotide in the HEK 293E-based *POT1* KO parental cell line (−/+ 4-OHT) and hPOT1-Myc WT or R83E complemented clonal cell lines treated with both 4-OHT and dox. (**C**) Quantitation of ATC-5' preference calculated as the ratio of the total band

Author Manuscript Author Manuscript Author Manuscript Author Manuscript

intensity in the primer 3 lane over the total intensity over all six lanes. Mean and SD for n=4 replicates of which B is representative are plotted. P-values were calculated using a two-tailed Student's t-test for comparisons against parental −4-OHT data (for parental +4-OHT) or hPOT1-Myc WT clones (for hPOT1-Myc R83E clones). (**D**) *Left:* Telomere restriction fragment (TRF) analysis of cell lines used in B performed first under native conditions with a 5'−^{32}P-labeled telomeric C-probe $(CTAACC)_4$ to detect the ss G-rich overhang. *Right:* Telomere restriction fragment (TRF) analysis after denaturing the DNA on the same gel and re-probing it to detect the total telomeric DNA signal; n=1. (**E**) Model for ATR inhibition at telomeres by POT1. The ss DNA-binding of hPOT1 prevents the loading of RPA to curb ATR recruitment to the 3' overhang. Protection of the ds-ss junction by hPOT1 prevents loading of the 9–1-1/Rad17-RFC clamp/clamp-loader complex and ATR activator TOPBP1. In mice, both POT1 paralogs coat the ss overhang but only POT1a protects the ds-ss junction. The shelterin proteins protecting the telomeric ds DNA are expected to keep POT1-TPP1 tethered to the ss overhang, facilitated by protein-protein interactions and the conformational flexibility within the proteins (29) and the telomeric DNA.